Lin, J.-W., Sugimori, M., Llinás, R. R., McGuinness, T. L., & Greengard, P. (1990) *Proc. Natl. Acad. Sci. U.S.A. 87*, 8257–8261.
Llinás, R., Gruner, J. A., Sugimori, M., McGuinness, T. L., & Greengard, P. (1991) *J. Physiol. (London) 436*, 257–282.
Llinás, R., McGuinness, T., Leonard, C. S., Sugimori, M., & Greengard, P. (1985) *Proc. Natl. Acad. Sci. U.S.A. 82*, 3035–3039.
Mandell, J. W., Townes-Anderson, E., Czernik, A. J., Cameron, R., Greengard, P., & De Camilli, P. (1990) *Neuron 5*, 19–33.
Mandell, J. W., Czernik, A. J., De Camilli, P., Greengard, P., & Townes-Anderson, E. (1992) *J. Neurosci.* (in press).
Morgan, D. O., Kaplan, J. M., Bishop, J. M., & Varmus, H. E. (1989) *Cell 57*, 775–786.
Nairn, A. C., & Greengard, P. (1987) *J. Biol. Chem. 262*, 7273–7281.
Nestler, E., & Greengard, P. (1983) *Protein Phosphorylation in the Nervous System*, Wiley, New York.
Okabe, T., & Sobue, K. (1987) *FEBS Lett. 213*, 184–188.
Peterson, G. (1977) *Anal. Biochem. 83*, 346–356.
Petrucci, T. C., & Morrow, J. S. (1987) *J. Cell. Biol. 105*, 1355–1363.
Piwnica-Worms, H. (1988) in *Current Protocols in Molecular Biology* (Ausubel, F. M., Brent, R., Kingston, R. E., Moore, D. D., Seidman, J. G., Smith, J. A., & Struhl, K., Eds.) pp 16.8.1–16.11.7, Greene Publishers and Wiley-Interscience, New York.
Schiebler, W., Jahn, R., Doucet, J.-P., Rothlein, J., & Greengard, P. (1986) *J. Biol. Chem. 261*, 8383–8390.
Sikorski, A. F., Terlecki, G., Zagon, I. S., & Goodman, S. R. (1991) *J. Cell Biol. 114*, 313–318.
Südhof, T. C., Czernik, A. J., Kao, H.-T., Takei, K., Johnston, P. A., Horiuchi, A., Kanazir, S. D., Wagner, M. A., Perin, M. S., De Camilli, P., & Greengard, P. (1989) *Science (Washington, D.C.) 245*, 1474–1480.
Summers, M. D., & Smith, G. E. (1987) *A Manual of Methods for Baculovirus Vectors and Insect Cell Culture Procedures*, Texas Agricultural Experiment Station Bulletin No. 1555, College Station, TX.
Thiel, G., Südhof, T. C., & Greengard, P. (1990) *J. Biol. Chem. 265*, 16527–16533.
Towbin, H., Staehelin, T., & Gordon, J. (1980) *Proc. Natl. Acad. Sci. U.S.A. 86*, 4350–4354.
Trimble, W. S., Gray, T. S., Elferink, L. A., Wilson, M. C., & Scheller, R. H. (1990) *J. Neurosci. 10*, 1380–1387.
Walaas, S. I., Girault, J.-A., & Greengard, P. (1989) *J. Mol. Neurosci. 1*, 243–250.
Wang, N. P., Qian, Y., Chung, A. E., Lee, W.-H., & Lee, E. Y.-H. P. (1990) *Cell Growth Differ. 1*, 429–437.

Luminescent/Paramagnetic Probes for Detecting Order in Biological Assemblies: Transformation of Luminescent Probes into π-Radicals by Photochemical Reduction†

Katalin Ajtai* and Thomas P. Burghardt
Department of Biochemistry and Molecular Biology, Mayo Foundation, Rochester, Minnesota 55905
Received September 12, 1991; Revised Manuscript Received February 10, 1992

ABSTRACT: The spectroscopic methods of fluorescence polarization and electron paramagnetic resonance (EPR) are used to study order and orientation of extrinsically labeled protein elements of ordered biological systems. These methods generate complementary information about the order of the system, but a consistent quantitative interpretation of the related data is complicated because the signals arise from different donors. We introduce a new method that allows us to detect both signals from the same donor. Unsubstituted xanthene dyes (eosin, erythrosin, and fluorescein) were irradiated by laser light at their absorption maximum in the presence of different reducing agents. Due to photochemical reduction, the quinoidal structure of the xanthene ring is transformed into a semiquinone, and a π-radical is formed having a characteristic EPR signal of an unpaired electron spin with proton hyperfine interactions. A strong EPR signal is observed from the dye in solution or when specifically attached to a protein following irradiation in the presence of dithiothreitol or cysteine. We applied this technique to the study of skeletal muscle fibers. The fluorescent dye (iodoacetamido)fluorescein was covalently attached to the reactive thiol of the myosin molecule in muscle fibers. Fluorescence polarization and EPR spectroscopy were performed on the labeled fibers in rigor. Both signals indicate a highly ordered system characteristic of cross-bridges bound to actin. Our use of the same signal donor for fluorescence and EPR studies of probe order is a promising new technique for the study of order in protein elements of biological assemblies.

The techniques of luminescence polarization and electron paramagnetic resonance (EPR) spectroscopy employing extrinsic probes are useful in quantitating orientation and order in biological assemblies because of their high sensitivity to differences or changes in probe orientation (Griffith & Jost, 1976; Arata & Shimizu, 1981; Morales et al., 1982; Gergely & Seidel, 1983; Vanderkooi & Berger, 1989). In the highly ordered skeletal muscle fiber system, two spatially separated points on the surface of the myosin cross-bridge, the reactive thiols SH1 and SH2, are routinely specifically modified by covalent probes of this type (Morales et al., 1982; Gergely & Seidel, 1983; Ajtai & Burghardt, 1989; Burghardt & Ajtai,

† This work was supported by the National Science Foundation (DMB 8819755), the National Institutes of Health (R01 AR 39288-01A2), the American Heart Association (Grant-in-Aid 900644), and the Mayo Foundation. T.P.B. is an Established Investigator of the American Heart Association.

0006-2960/92/0431-4275$03.00/0

1990). Luminescent and paramagnetic probes of myosin cross-bridges can indicate cross-bridge orientation and are used to study cross-bridge orientation changes during muscle contraction. Previously, probe orientation data collected from different probes of SH1 were interpreted as indicating contradictory extents of cross-bridge rotation in fibers. Some probes of SH1 were said to indicate a large cross-bridge rotation when the fiber changes its physiological state while others were said to indicate almost no change under identical conditions (Cooke et al., 1982; Ajtai & Burghardt, 1986; Ajtai et al., 1989; Fajer et al., 1990). These contradictions are from both the complexity of the three-dimensional structure of the active cross-bridge (i.e., that the cross-bridge is probably not strictly a rigid body undergoing a rotation during muscular contraction) and the difficulty in comparing data originating from different signal donors on SH1. We suggest that these difficulties in interpreting probe data are common problems in probe studies of order and orientation in biological assemblies.

We address the latter difficulty here by introducing a new application of probes that are both luminescent and paramagnetic. A family of luminescent probes made from an unsubstituted xanthene dye are reduced to a free radical when they absorb a photon in the presence of specific reducing agents (Oster & Adelman, 1956; Adelman & Oster, 1956; Uchida et al., 1959; Grossweiner & Zwicker, 1959, 1961; Zwicker & Grossweiner, 1963; Kasche & Lindquist, 1965; Kasche, 1967). The kinetics of this photochemical process are slow enough at low excitation light levels that luminescence polarization spectroscopy measurements can be made without appreciable probe photobleaching or photoreduction to the free radical. Free radical formation is appreciable at the higher excitation light levels such that a characteristic EPR signal is observed under these conditions.

Previously, we developed a method for mapping global angular transitions of proteins in assemblies using multiple fluorescent and spin probes (Burghardt & Ajtai, 1992; Ajtai et al., 1992). This method searches for (and treats as an unknown) the relationship between the principal magnetic frame of the spin probe and the absorption dipole of the fluorescent probe. In the case of our luminescent/paramagnetic probes, we will show below that this relationship can be determined directly from the EPR spectrum. Thus, the use of a luminescent/paramagnetic probe can potentially reduce the number of unknowns and thereby the ambiguity in interpreting probe data.

We developed our method specifically to detect the orientation of probes on the myosin cross-bridges of muscle fibers. With it we are able to measure the fluorescence polarization and EPR spectrum from the same probe under identical conditions. Both spectra indicate a highly ordered assembly of probes characteristics of cross-bridges in muscle fibers. With this application, we demonstrate the utility of the luminescent/paramagnetic probes.

Materials and Methods

Chemicals. ATP, trypsin, and chymotrypsin were from Sigma (St. Louis, MO). The dyes fluorescein, eosin, and erythrosin were from Eastman Kodak (Rochester, NY). 5-(Iodoacetamido)fluorescein (IAF) was from Molecular Probes (Eugene, OR). All chemicals were analytical grade.

Solutions. Rigor solution contained 80 mM KCl, 5 mM $MgCl_2$, 2 mM EGTA, 5 mM potassium phosphate, and 4 mM dithiothreitol (DTT) at pH 7. Relaxing solution was rigor solution with 4 mM MgATP. Solutions containing glycerol consisted of rigor or relaxing solution with glycerol added volume-to-volume to obtain the desired percent glycerol concentration at pH 7.

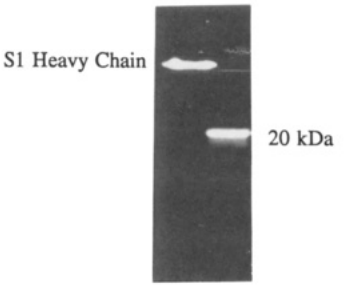

FIGURE 1: SDS–PAGE of F-S1 (lane 1, left) and tryptic F-S1 (lane 2, right). Lane 2 contains the characteristic 50-, 27-, and 20-kDa fragments of which only the 20-kDa fragment is labeled.

Preparation and Labeling of Proteins. Rabbit myosin was prepared by the standard method (Tonomura et al., 1966). Myosin subfragment 1 (S1) was obtained by digesting myosin filaments with α-chymotrypsin (Weeds & Taylor, 1975). The S1 was labeled with a 1.2-fold molar excess of IAF in 50 mM TES, pH 7 at 4 °C, in the dark for 24 h. The reaction was stopped by adding 1 mM DTT. The unreacted dye was removed by gel filtration.

Localization of the probe in the proteolytic fragments of S1 was carried out using sodium dodecyl sulfate–polyacrylamide gel electrophoresis (SDS–PAGE) on the tryptic digest of fluorescein-labeled S1 (F-S1) (Bálint et al., 1975). Shown in Figure 1 are fluorescent images of an SDS–PAGE experiment on F-S1 (lane 1, left) and tryptic F-S1 (lane 2, right). Tryptic proteolysis of F-S1 produces three characteristic fragments of 50, 27, and 20 kilodalton (kDa) molecular mass. SH1 residues in the 20-kDa fragment (Bálint et al., 1978). The fluorescein, localized in the heavy chain of F-S1 in lane 1, migrates with the 20-kDa fragment of tryptic F-S1 in lane 2, suggesting fluorescein modified SH1 in S1.

The fluorescein molar extinction coefficient of 6.8×10^4 (λ_{ex} = 499 nm) was used to directly estimate the amount of protein-bound dye from the absorption spectrum. For F-S1, the number of probes per protein was determined to be 0.63 ± 0.05. In enzymatic activity measurements, the characteristic alteration of myosin S1 ATPase upon SH1 modification, such that modification of SH1 causes a linear inhibition of K^+-EDTA ATPase activity, was used to estimate SH1 modification. The number of reacted SH1 groups per protein was determined to be 0.59 ± 0.05. The percent difference of probes per protein and reacted SH1's per protein is within the experimental error of the measurements. These data, taken with the finding that fluorescein labels only the 20-kDa tryptic fragment of F-S1 (see Figure 1), indicate that fluorescein specifically modifies SH1.

We studied the effect of radical formation at SH1 on the nativity of S1 by measuring the ATPase rate of F-S1 in solution before and after illumination and detection of the EPR spectrum. We found identical K^+-EDTA or Ca^{2+} ATPases for the F-S1 in both cases, suggesting the protein remains native under these conditions.

Preparation and Labeling of Muscle Fibers. We obtained rabbit psoas muscle fibers as described previously (Borejdo et al., 1979) and stored them in relaxing solution containing 50% glycerol at −15 °C for up to several weeks. Small bundles of skinned fibers were labeled with 120 μM IAF in relaxing solution (without DTT) for 30 min at 4 °C with intense stirring. The reaction was stopped with 1 mM DTT, and the excess of the dye was washed out with relaxing solution. We checked probe specificity with a protocol analogous to that

used with F-S1 by extracting the myosin from the labeled muscle fibers and visualizing the IAF-labeled proteins extracted from the fiber and separated by gel electrophoresis, and by measuring the probe absorption spectrum and characteristic alteration of myosin ATPase upon SH1 modification (Ajtai & Burghardt, 1989). We found that 35% of the myosin heads in the fiber were covalently labeled and that ~80% of the total amount of IAF was located at SH1. The remaining ~20% was distributed among α-actinin, actin, and myosin light chain 1.

We studied the effect of probe modification of SH1 and subsequent radical formation on the nativity of the contractile apparatus by measuring rigor tension before modification with IAF, after modification but before illumination to cause radical formation, and after radical formation. We found identical rigor tension in each case, suggesting the fiber remains native under these conditions.

EPR Measurements. EPR measurements were carried out at X-band on a Bruker Model ER200 series instrument using a TM_{110} cylindrical cavity. For these measurements, we continuously illuminated samples inside the EPR cavity with monochromatic light from an argon ion laser propagating at right angles to the Zeeman field. The excitation wavelengths used were near the absorption maximum of the dye, i.e., 488 nm with fluorescein or 514 nm with eosin or erythrosin. The laser beam was circularly polarized and slightly expanded to illuminate an area of 1 cm^2 inside the cavity. No EPR signal was observed without light excitation, and the shape of the spectra was unaffected by the presence of oxygen.

The EPR signal from continuously illuminated probe-labeled samples followed a time course in which immediately after the excitation light was turned on the signal rose to a constant steady-state value within 1 min. The steady-state signal level remained constant for ≥10 min for all samples tried and then slowly declined because of the depletion of the unbleached probes. We collected the EPR spectrum from samples only during the constant phase of the signal level.

We fitted spectra from the immobilized labeled proteins using a spin Hamiltonian appropriate for a radical in a large Zeeman field with a hyperfine interaction from two equivalent protons. The appropriate Hamiltonian, H, is given by

$$H = \beta_e \mathbf{H}\cdot\mathbf{g}\cdot\mathbf{S} + g_e\beta_e\mathbf{I}\cdot\mathbf{T}\cdot\mathbf{S} \quad (1)$$

where β_e is the Bohr magneton, g_e is a scalar equal to the g-factor of a free electron, **H** is the Zeeman field, **S** is the spin operator for the unpaired electron, **I** is the total nuclear spin of the two equivalent protons, **g** is the anisotropic **g**-"tensor", and **T** is the anisotropic **T**-"tensor". The energy levels of this system are approximately calculated to lowest order in the hyperfine interaction using perturbation theory (Merzbacher, 1970; Abragam & Bleany, 1970). The resonance condition requires that

$$H_0 = g_e\left\{\frac{h\nu}{\beta g_e} + \frac{m_I|\mathbf{k}\cdot\mathbf{T}|}{|\mathbf{k}\cdot\mathbf{g}|}\right\}\Big/|\mathbf{k}\cdot\mathbf{g}| \quad (2)$$

where H_0 is the resonant Zeeman field, $h\nu$ is the microwave energy, $m_I = 1, 0, -1$ is the nuclear spin projection quantum number, and **k** is the unit vector parallel to the Zeeman field. The scalar quantities $|\mathbf{k}\cdot\mathbf{T}|$ and $|\mathbf{k}\cdot\mathbf{g}|$ are defined by

$$|\mathbf{k}\cdot\mathbf{g}| \equiv [(k_1g_x)^2 + (k_2g_y)^2 + (k_3g_z)^2]^{1/2} \quad (3)$$

$$|\mathbf{k}\cdot\mathbf{T}| \equiv [(k_1T_xg_x)^2 + (k_2T_yg_y)^2 + (k_3T_zg_z)^2]^{1/2} \quad (4)$$

For the approximation used to find eq 2, the transition probability for microwave photon absorption is the same for all lines and mildly dependent on probe orientation.

The EPR spectrum for immobilized probes, $F(H)$, is given by

$$F(H) = \int_{\Omega_0} d\Omega\ (\mathbf{E}\cdot\mu_a)^2 N(\Omega) \sum_{m_I=-1}^{1} b_{mI} \exp\{-(\ln 2)(H - H_0)^2/\epsilon_{mI}^2\} \quad (5)$$

where Ω represents the Euler angles (α, β, γ) describing the orientation of the principal magnetic frame of the probe relative to the lab-fixed frame, Ω_0 is the domain $0 \le \alpha_0 \le 2\pi$, $0 \le \beta_0 \le \pi$, and $0 \le \gamma_0 \le 2\pi$, **E** is the electric field of the excitation light, μ_a is the absorption dipole of the probe, $N(\Omega)$ is the probe angular distribution, b_{mI} is the angular-dependent microwave absorption probability, ϵ_{mI} is the line width for the m_I'th line, and the lineshape is Gaussian. The $m_I = 0$ resonance line corresponds to two equally likely transitions so that $b_0 = 2b_1$ while $b_1 = b_{-1}$. The Euler angles α and β are the probe azimuth and polar angles relative to the fiber symmetry axis, and γ is the torsion angle (Davydov, 1963). Equations 3 and 4 presume the molecular frame of the probe to be the principal magnetic frame. In this case, μ_a is a general unit vector of the form

$$\mu_a = (\sin\theta_a\cos\phi_a, \sin\theta_a\sin\phi_a, \cos\theta_a) \quad (6)$$

where θ_a and ϕ_a are the polar and azimuthal angles of the vector, respectively.

The probe angular distribution, $N(\Omega)$, is expanded in terms of orthonormal functions on the interval Ω_0 such that

$$N(\Omega) = \sum_{j=0}^{j_{max}} \sum_{m,n=-j}^{j} a^j_{m,n}\sqrt{(2j+1)/8\pi^2}\ \mathbf{D}^j_{m,n} \quad (7)$$

where $a^j_{m,n}$ is an order parameter of rank j and $\mathbf{D}^j_{m,n}$ is a Wigner matrix element (Davydov, 1963). For EPR measurements, $a^j_{m,n} = 0$ unless $m = 0$, $j = 0, 2, 4, \ldots$, and $n = 0, 2, 4, \ldots, j$. The maximum rank of order parameter that contributes significantly to the EPR spectrum is j_{max} (Burghardt & French, 1989).

Fluorescence Polarization Measurements. Fluorescence measurements were performed on an SLM 8000 spectrofluorometer (SLM Instruments, Urbana, IL) equipped with Glan–Thompson polarizers. The emission was collected at 90° from the excitation beam path. The emission wavelength was selected with a band-pass filter transmitting a wavelength band of 10 nm centered at $\lambda_{em} = 550$ nm.

The fluorescence polarization experiment on a labeled fiber consisted of measuring the fluorescent intensities $F_{\parallel,\parallel}$, $F_{\parallel,\perp}$, $F_{\perp,\perp}$, and $F_{\perp,\parallel}$ where $\parallel$ or $\perp$ refers to light polarization measured relative to the fiber axis and the first index refers to excitation, the second to emission. We oriented the fiber so that the fiber axis was perpendicular to both the excitation and collected emission beam paths. The fluorescent intensities have identical but arbitrary normalizations so they are combined into ratios, $P_\parallel$, $P_\perp$, and $Q_\parallel$, defined by

$$P_\parallel \equiv (F_{\parallel,\parallel} - F_{\parallel,\perp})/(F_{\parallel,\parallel} + F_{\parallel,\perp}) \quad (8)$$

$$P_\perp \equiv (F_{\perp,\perp} - F_{\perp,\parallel})/(F_{\perp,\perp} + F_{\perp,\parallel}) \quad (9)$$

$$Q_\parallel \equiv (F_{\parallel,\parallel} - F_{\perp,\parallel})/(F_{\parallel,\parallel} + F_{\perp,\parallel}) \quad (10)$$

We summarize our data by plotting $P_\parallel$, $P_\perp$, and $Q_\parallel$ as functions of excitation wavelength. For a random distribution of immobilized probes, $P_\parallel(\lambda_{ex})$ indicates the angle between the absorption and emission dipoles of the probe and $P_\perp(\lambda_{ex}) = 0$.

The fluorescence polarization experiments on F-S1 in solution consisted of measuring $P_\parallel$ or the anisotropy, r, defined by

$$r \equiv (F_{\parallel,\parallel} - F_{\parallel,\perp})/(F_{\parallel,\parallel} + 2F_{\parallel,\perp}) \quad (11)$$

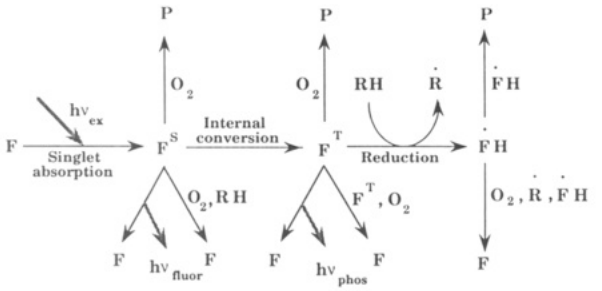

FIGURE 2: Mechanism for the photoreduction of light-absorbing dye, F (corresponding to fluorescein, eosin, or erythrosin), by the reducing agent RH. After absorption of a photon of frequency ν_{ex}, the dye is in its excited singlet state, F^S, and can return to a lower energy state by (i) interacting with oxygen to either form nonabsorbing products (P) (i.e., become irreversibly bleached) or become quenched, (ii) becoming quenched by the reducing agent RH, (iii) fluorescing at frequency ν_{fluor}, or (iv) undergoing internal conversion to the triplet state, F^T. The triplet state can decay to a lower energy state by several paths including irreversible photobleaching, triplet quenching, or light emission (phosphorescence). Reduction to the radical form, FH, takes place from the triplet state by the oxidation of RH. The free radical, FH, also has several mechanisms for returning to a lower energy state including bleaching and quenching.

with emission collected as with labeled fibers. The low-temperature experiments were performed in rigor plus 50% or 66.6% glycerol. At the 66.6% glycerol concentration, the freezing point of the solution is depressed to ≤−45 °C (Miner & Dalton, 1953).

Results and Discussion

We report here studies of fluorescein and its halogenated derivatives eosin and erythrosin. Eosin and erythrosin have a high efficiency for excited singlet- to triplet-state conversion when in solution (Bowers & Porter, 1967). The lifetime of the triplet is many orders of magnitude longer than the singlet state, and in these two probes, the quantum efficiency for phosphorescent emission is significant. Because of these properties, eosin and erythrosin, when modified to react with specific side chains of proteins, are used to detect rotational relaxation rates of their protein hosts using time-resolved optical techniques (Ludescher et al., 1987). The longer lifetime of the triplet probes allows investigation of slower relaxation rates than is possible with singlet probes. Fluorescein has a lower efficiency for triplet conversion and in most applications is used as a fluorescent probe of proteins in biological assemblies.

The chemistry of the photoreduction of these dyes was studied by measuring steady-state or time-resolved absorption following flash or continuous illumination photolysis (Zwicker & Grossweiner, 1963) as well as with EPR measurements of the radical intermediates (Bubnov et al., 1959). Figure 2 gives a general scheme for the photoreduction of these dyes that is a summary of several investigations over many years. In time-resolved experiments, studies of the kinetics of the dye reaction were conducted with phenol as the reducing agent (Zwicker & Grossweiner, 1963). From these studies, it was proposed that the dye was reduced from its triplet state by electron transfer from phenol, producing free radical forms of both the dye and the phenol.

Subsequent work using EPR to detect radical intermediates from eosin and phenol in methanol, following illumination by a flash of visible light in the presence of oxygen, showed that not the phenoxy radical but its product from further reaction with the reduced eosin was detected (Leaver, 1971). This product, the *p*-benzosemiquinone anion radical, has a characteristic five-line EPR spectrum due to an unpaired electron interacting with four equivalent protons. The relative intensity of the lines is given by the ratios 1:4:6:4:1 (Venkataraman et al., 1959). In this case, the reduced eosin free radical was not detected because of its rapid reaction with the phenoxy radical. We also observed the production of *p*-benzosemiquinone with EPR from eosin and phenol in phosphate buffer (pH 7.0) under constant illumination from the 514-nm line from an argon ion laser (data not shown).

In other previous work, the reduced dye free radical was detected using EPR from eosin and ascorbic acid in pyridine in the absence of oxygen and under constant illumination with visible light (Bubnov et al., 1959). The ascorbic acid served as the reducing agent. The EPR spectrum obtained had three lines with a hyperfine splitting of 4.6 G. The ratio of the intensity of the components of the hyperfine structure was 1:2:1. The proposed detailed mechanism for the formation of the reduced eosin free radical is summarized in Figure 3. The unpaired π-electron of the eosin must interact with two protons at equivalent positions in the molecule to give the relative intensity of the components of the hyperfine structure of 1:2:1. These protons are at positions 8 and 1 in rings a and c, respectively.

We performed similar experiments with fluorescein, eosin, and erythrosin. We modified the known conditions for the photoreduction of the dyes to be able to use the method on biological systems. We used DTT or cysteine as reductants because these antioxidants do not denature the proteins. DTT and cysteine reduced the probes free in solution and when the probes were covalently bound to proteins or protein assemblies and did not disturb the activity of the biological system. All of our experiments were conducted in buffered solution at pH 7.0 and containing 4 mM DTT or cysteine.

EPR spectra from these dyes freely moving in solution are shown in Figure 4. The spectra have the general hyperfine features of an unpaired electron interacting with two equivalent protons as discussed above. Additional weaker hyperfine interactions, that are not fully resolved, split the original three lines, suggesting an interaction with a different set of four approximately equivalent protons. These protons are possibly those in the d ring of the molecule shown in Figure 3. We do not observe any EPR signal originating from the apparently oxidized DTT or cysteine. We found that of the (iodoacetamido)xanthene dyes, the fluorescein dye reacted most specifically with the SH1 group of myosin and therefore we chose (iodoacetamido)fluorescein (IAF) to use in our study of labeled myosin.

Shown in Figure 5 are EPR spectra from fluorescein-labeled myosin subfragment 1 (F-S1) at 4 °C (top) and in 50% glycerol at −15 °C (bottom). The effect of the rapidity of dye rotation on the shape of the EPR spectrum is seen by comparing spectra from fluorescein in solution (Figure 4) to those from F-S1 free in solution (Figure 5, top). The spectra from the rapidly mobile probes are narrowed so that the relative intensity 1:2:1 lines are well resolved and the quintet splittings are less resolved but clearly present. The slowly moving probes have a broadened EPR spectrum with overlapping lines. The broadening is pronounced enough to suppress most of the features of the hyperfine splittings.

The EPR spectrum from F-S1 in solution at 4 °C is indicative of a slowly rotating probe with a rotational relaxation time between that of a free probe and the immobilized probe (but closer to that of the immobilized probe, comparing Figure 4 with Figure 5). The hyperfine extrema from F-S1 in solution, $\Delta H = 10.0 \pm 0.1$ G, is only slightly smaller than that from immobilized F-S1, $\Delta H = 10.2 \pm 0.1$ G, suggesting that

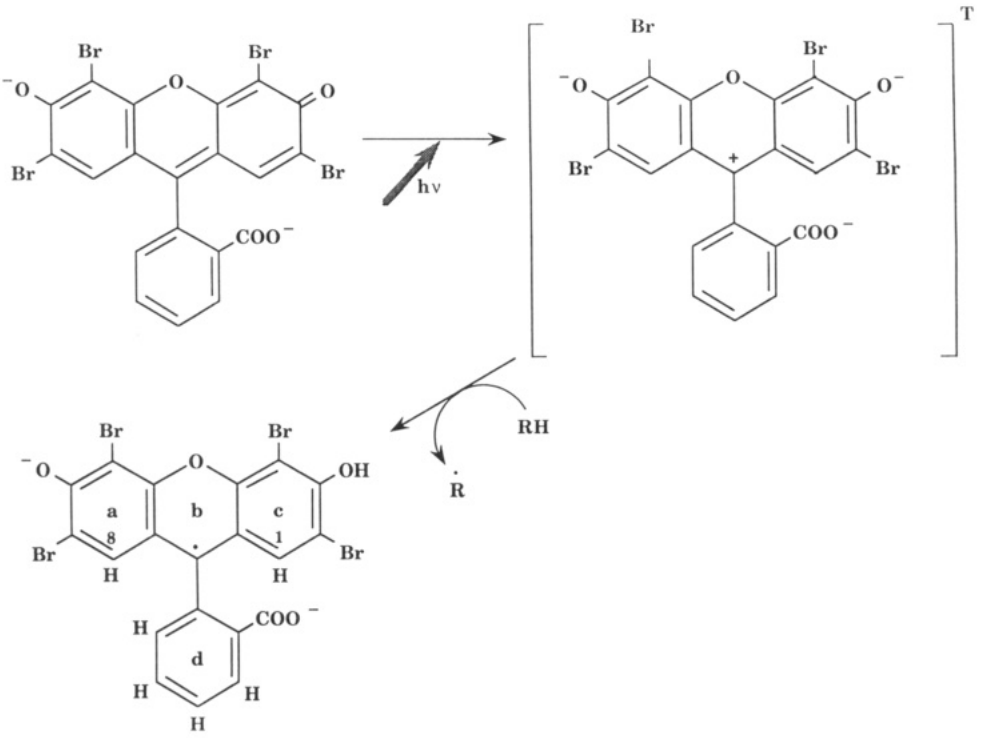

FIGURE 3: Detailed mechanism for the photoreduction of eosin. The diagram shows the π-radical form of eosin and the equivalent protons at carbons 8 and 1 causing the three well-resolved lines in the EPR spectra shown in Figure 4. The additional quintet of hyperfine splitting may be due to the protons in the d ring. We presume that an identical mechanism is responsible for the photoreduction of fluorescein.

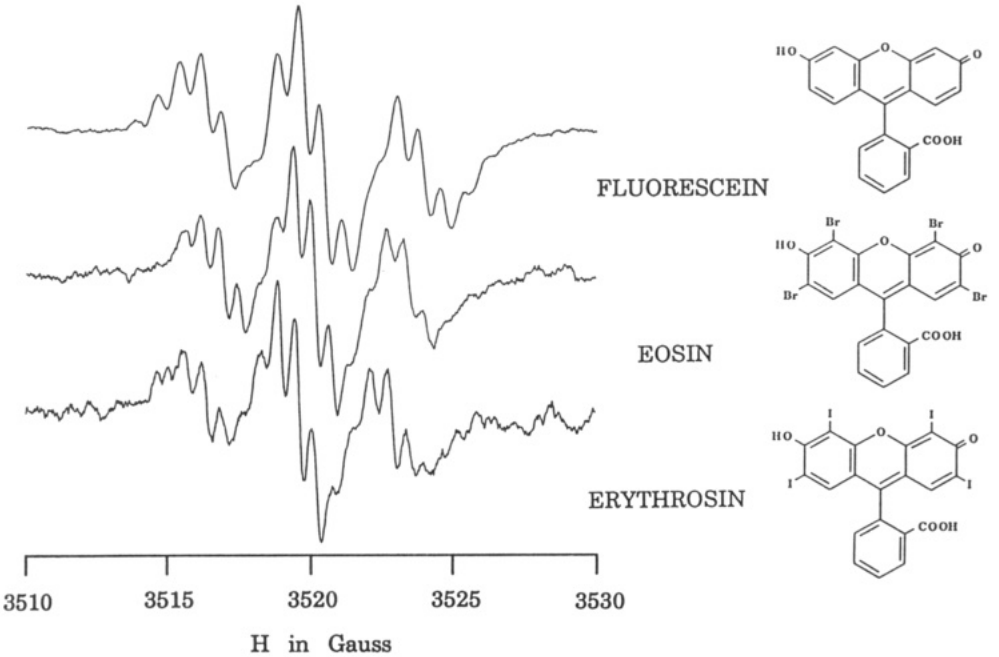

FIGURE 4: EPR spectra from 0.2 mM fluorescein, eosin, and erythrosin in 4 mM DTT/5 mM phosphate buffer, pH 7.0, and at room temperature. EPR was measured with 1-mW microwave power and 0.5-G modulation amplitude. Laser illumination power was continuous at 100 mW. The hyperfine splittings are from a set of two nearby equivalent protons, giving the characteristic three lines in the intensity relationship of 1:2:1, and a more distant set of four approximately equivalent protons that split each line into a quintet.

the fluorescein probe on the surface of S1 is immobilized on the time scale of the spin relaxation and that the indicated slow rotational motion of F-S1 in solution is from the rotation of the F-S1 complex. EPR spectra from F-S1 in buffer at 4 °C in the presence of the nucleotides MgATP and MgADP (data not shown) are identical to the spectrum shown in Figure 5 (top) in the absence of nucleotides. This observation suggests that substrate binding to S1 does not mobilize the label, making IAF a potentially reliable probe for detecting myosin cross-bridge orientation changes in fibers in various physiological states including contraction. This observation does not necessarily conflict with previous observations of fluorescence intensity changes from F-S1 under similar conditions (Ando, 1984; Aguirre et al., 1986).

We investigated the EPR spectrum from an immobilized and oriented distribution by fluorescein labeling SH1 on myosin cross-bridges in glycerinated muscle fibers. These spectra, shown in Figure 6, are from IAF-labeled fibers in rigor that are oriented with the fiber axis parallel (top) or perpendicular (bottom) to the Zeeman field. Comparison of these spectra shows the sensitivity of the shape of the signal to changes in probe orientation.

FIGURE 5: EPR spectra from F-S1 in 4 mM DTT and 25 mM TES buffer, pH 7, at 4 °C (top) and from F-S1 in rigor + 50% glycerol at −15 °C (bottom). Protein concentration was 100 μM with 0.7 probe per S1. EPR was measured with 1-mW microwave power, 2.0-G modulation amplitude, and 150-mW continuous laser power. The solid line in the lower spectrum is the best fitting theoretical curve obtained by using a random distribution of probes and the following spectral parameters (defined in eq 1–6): $g_x = 2.0083 \pm 0.0002$, $g_y = 2.0051 \pm 0.0002$, $g_z = 2.0019 \pm 0.0002$, $T_x = 2.8 \pm 0.2$ G, $T_y = 5.0 \pm 0.2$ G, $T_z = 1.9 \pm 0.2$ G, $\epsilon_{-1} = 4.0 \pm 0.2$ G, $\epsilon_0 = 1.6 \pm 0.2$ G, $\epsilon_1 = 3.9 \pm 0.2$ G, $\theta_a = 105 \pm 2°$, and $\phi_a = 0 \pm 2°$.

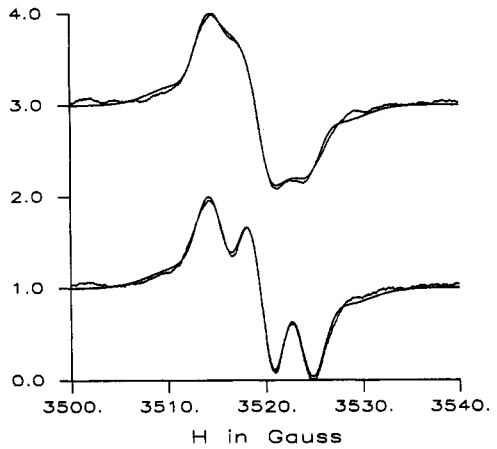

FIGURE 6: EPR spectra from IAF-labeled muscle fibers at 4 °C in rigor oriented either parallel (top) or perpendicular (bottom) to the Zeeman field. In both cases, fiber axes were perpendicular to the propagation direction of the illuminating light. EPR experimental parameters were identical to those mentioned in Figure 5. The solid line in each spectrum is the best fitting theoretical curve.

We fitted the EPR spectrum from F-S1 in 50% glycerol at −15 °C with eq 5 and a random distribution of probes. We varied the spectral parameters **g**, **T**, and ϵ_{ml} and the orientation of μ_a in the principal magnetic frame to best fit the spectrum. Using the spectral parameters so determined, we fitted the EPR spectrum from fluorescein-labeled muscle fibers using eq 5 to obtain the probe angular distribution, $N(\Omega)$. The fit to the EPR spectrum, shown by the solid line of Figure 6, deviates from the experimental curve in the low- and high-field regions of the spectrum. We considered EPR spectra from many different labeled muscle fibers and determined that these deviations are smaller than the differences between spectra obtained from different labeled fibers. Additionally, in regions where the EPR signal is small, base-line anomalies contribute a greater fraction of the total signal compared to regions where the sample EPR signal is different from zero. Consequently, we believe that the deviations between measured and simulated spectra are incidental and do not necessarily imply eq 5 (and the assumptions leading to it) is incorrect or incomplete.

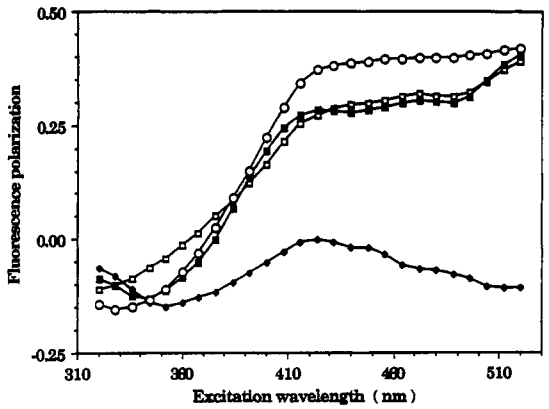

FIGURE 7: Fluorescence polarization excitation spectra from IAF-labeled fibers in rigor and from F-S1 in rigor + 50% glycerol at −15 °C [(○) $P_\parallel$ random]. Polarization ratios $P_\parallel$ (□), $P_\perp$ (♦), and $Q_\parallel$ (■) are defined in eq 8–10.

The fluorescein label, used in the EPR studies, was also used in fluorescence polarization studies. We conducted fluorescence polarization experiments on F-S1 in rigor at 4 °C, in rigor + 50% glycerol at −15 °C, and in rigor + 66.6% glycerol at temperatures ranging from −15 to −45 °C. In rigor buffer at 4 °C, we obtained a peak polarization anisotropy from F-S1 of $r_{sol} = 0.303 \pm 0.003$. In rigor + 50% glycerol, the peak anisotropy of F-S1 was $r_{imm} = 0.337 \pm 0.007$. In 50% glycerol at −15 °C, an independently mobile probe the size of fluorescein is expected to move with a rotational relaxation time of ~50 ns. This motion is rapid enough to be detected by steady-state fluorescence polarization and would become a factor of 10^3 slower in 66.6% glycerol at −45 °C. F-S1 in 50% glycerol at −15 °C or in 66.6% glycerol at −45 °C gives identical peak anisotropies, indicating that the fluorescein probe is immobilized on the surface of S1 on the time scale of the fluorescence lifetime under these conditions.

The decrease in anisotropy from r_{imm} to r_{sol} reflects principally the independent motion of the fluorescein on S1 because S1 rotational relaxation contributes only 5% of the depolarization during the 4.5-ns lifetime of the probe. The anisotropy decrease from independent probe motion is equivalent to allowing the probe to move rapidly (compared to the lifetime) through an angle of 11.6° (Lakowicz, 1983). We have not attempted to correct our simulated EPR spectra for contributions from the radical probes moving rapidly through this negligibly small independent angular degree of freedom. These data support the conclusion that, for practical purposes, fluorescein is immobilized on the surface of S1.

The fluorescence polarization excitation spectra from fluorescein-labeled muscle fibers in rigor and from F-S1 in 50% glycerol at −15 °C are shown in Figure 7. The polarization ratios $P_\parallel$, $P_\perp$, and $Q_\parallel$ are defined in eq 8–10. Spectra from immobilized randomly distributed F-S1 have ratios $Q_\parallel = P_\parallel$ and $P_\perp = 0$. Comparison of the polarization ratios from the labeled fibers to those from immobilized randomly distributed F-S1 indicates that the probes labeling the muscle fiber are ordered as expected from the EPR results.

The probe angular distribution, $N(\Omega)$, for fluorescein-labeled fibers, derived exclusively from the EPR spectrum using eq 5, is shown in Figure 8. The plot is lower in angular resolution than is typical for conventional nitroxide probes due mainly to the low anisotropy of the T-"tensor" in the hyperfine coupling term of eq 1. We found that the maximum rank of order parameter that contributed significantly to the EPR spectrum, defined as j_{max} in eq 7, was 12. With nitroxide probes, $j_{max} \geq 16$ is typical. We showed, with a different system, that we may increase the angular resolution of the probe angular

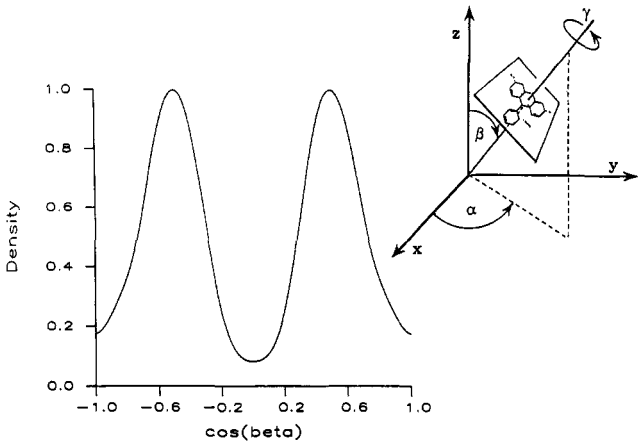

FIGURE 8: Probe angular distribution, $N(\Omega)$, integrated over Euler angles α and γ and plotted as a function of cos β. The insert indicates the Euler angles relating the laboratory frame (x, y, z) with the principal magnetic frame of the probe. The fiber axis of symmetry lies parallel to the actin filament and along the lab z-axis.

distribution by combining EPR with the fluorescence polarization data, but we have not yet carried out this calculation on the EPR and fluorescence polarization data from fluorescein-labeled fibers (Burghardt & Ajtai, 1992; Ajtai et al., 1992). Nevertheless, the low-resolution distribution shows a maximum at $\beta = 60°$, indicating that the fluorescein is oriented on the cross-bridge in a direction that was not investigated before by spin-labels. This may prove to be another advantage of the fluorescein in the investigation of cross-bridge order and orientation. Future studies using this probe will investigate cross-bridge orientation changes as a result of physiological state changes in the muscle fiber.

Conclusions

Our approach that utilizes one chemical group as a luminescent and paramagnetic probe permits us to detect the orientation changes of protein components of the biological assembly, to a degree exceeding that available by introducing two conventional probes, but with the advantage that only one protocol for the specific and unharmful modification of the protein need be found. This approach also allows us to experiment on a labeled biological sample that is closer to its native state than if nitroxide-labeled samples were used. This is because the conventional nitroxide spin-label requires conditions that protect the radical from undergoing unwanted oxidation or reduction so that the routine use of antioxidants, such as DTT or mercaptoethanol, to protect the native structure of proteins by preventing disulfide bridge formation is not permitted. Thus, the conditions consistent with the measurement of fluorescence or the photoreduction of our xanthene dyes are better for protecting the integrity of the protein structure than the conventional nitroxide spin-label methods.

We demonstrated the use of fluorescein as a signal donor for both fluorescence and EPR studies of probe order and orientation in glycerinated muscle fibers. This approach provides two complementary signals related to probe order and orientation that can be applied to native biological assemblies. Other unexplored applications of this method include EPR studies of dynamic or steady-state systems using linearly polarized and/or wavelength varying excitation light to generate the π-radicals. Linearly polarized light will generate radicals with absorption dipoles preferentially aligned with the light polarization. Also, the orientation of absorption dipoles within the probe can be changed by varying the excitation wavelength. Consequently, an oriented ensemble of π-radicals, that is a subset of the probe population, can be created by adjusting light polarization and/or wavelength in our system. We used this property previously to investigate selected degrees of rotational freedom in cross-bridges with wavelength-dependent fluorescence polarization applied to labeled muscle fibers (Ajtai & Burghardt, 1987). Our new technique extends these properties, characteristic of luminescence spectroscopy, to the EPR spectroscopy of spin-labels.

Acknowledgments

We thank N. Simmons and D. J. Toft for excellent technical assistance, A. Ringler for help in preparing the manuscript, and E. H. Hellen, P. J. K. Ilich, and F. G. Prendergast for helpful discussions.

Registry No. IAF, 63368-54-7; eosin, 17372-87-1; erythrosin, 16423-68-0; fluorescein, 2321-07-5.

References

Abragam, A., & Bleaney, B. (1970) *Electron Paramagnetic Resonance of Transition Ions*, p 168, Dover, New York.
Adelman, A. H., & Oster, G. (1956) *J. Am. Chem. Soc. 78*, 3977–3980.
Aguirre, R., Gonsoulin, F., & Cheung, H. C. (1986) *Biochemistry 25*, 6827–6835.
Ajtai, K., & Burghardt, T. P. (1986) *Biochemistry 25*, 6203–6207.
Ajtai, K., & Burghardt, T. P. (1987) *Biochemistry 26*, 4517–4523.
Ajtai, K., & Burghardt, T. P. (1989) *Biochemistry 28*, 2204–2210.
Ajtai, K., French, A. R., & Burghardt, T. P. (1989) *Biophys. J. 56*, 535–541.
Ajtai, K., Ringler, A., & Burghardt, T. P. (1992) *Biochemistry 31*, 207–217.
Ando, T. (1984) *Biochemistry 23*, 375–381.
Arata, T., & Shimizu, H. (1981) *J. Mol. Biol. 151*, 411–437.
Bâlint, M., Srêter, F., Wolf, I., Nagy, B., & Gergely, J. (1975) *J. Biol. Chem. 250*, 6177–6188.
Bâlint, M., Wolf, I., Tarcsafalvi, A., Gergely, J., & Srêter, F. (1978) *Arch. Biochem. Biophys. 190*, 793–799.
Borejdo, J., Putnam, S., & Morales, M. F. (1979) *Proc. Natl. Acad. Sci. U.S.A. 76*, 6346–6350.
Bowers, P. G., & Porter, G. (1967) *Proc. R. Soc. London, A 299*, 348–353.
Bubnov, N. N., Kibalko, L. A., Tsepalov, V. F., & Shliapintokh, V. IA. (1959) *Opt. Spectrosc. (Engl. Transl.) 7*, 71–72.
Burghardt, T. P., & French, A. R. (1989) *Biophys. J. 56*, 525–534.
Burghardt, T. P., & Ajtai, K. (1990) in *Molecular Mechanism in Muscle Contraction* (Squire, J. M., Ed.) Vol. 3, pp 211–239, MacMillan, London.
Burghardt, T. P., & Ajtai, K. (1992) *Biochemistry 31*, 200–206.
Cooke, R., Crowder, M. S., & Thomas, D. D. (1982) *Nature (London) 300*, 776–778.
Davydov, A. S. (1963) *Quantum Mechanics*, p 145, NEO Press, Ann Arbor, MI.
Fajer, P. G., Fajer, E. A., Matta, J. J., & Thomas, D. D. (1990) *Biochemistry 29*, 5865–5871.
Gergely, J., & Seidel, J. C. (1983) *Handb. Physiol., Sect. 10*, 257–274.
Griffith, O. H., & Jost, P. C. (1976) in *Spin Labeling: Theory and Applications* (Berliner, L. J., Ed.) Vol. I, pp 453–523, Academic Press, New York.

Grossweiner, L. I., & Zwicker, E. F. (1959) *J. Chem. Phys. 31*, 1141-1142.
Grossweiner, L. I., & Zwicker, E. F. (1961) *J. Chem. Phys. 34*, 1411-1417.
Kasche, V. (1967) *Photochem. Photobiol. 6*, 643-650.
Kasche, V., & Lindquist, L. (1965) *Photochem. Photobiol. 4*, 923-933.
Lakowicz, J. R. (1983) in *Principles of Fluorescence Spectroscopy*, p 136, Plenum, New York.
Leaver, I. H. (1971) *Aust. J. Chem. 24*, 891-894.
Ludescher, R. D., Eads, T. M., & Thomas, D. D. (1987) in *Optical Studies of Muscle Cross-Bridges* (Baskin, R. J., & Yeh, Y., Eds.) pp 33-65, CRC Press, Boca Raton, FL.
Merzbacher, E. (1970) *Quantum Mechanics*, p 413, Wiley, New York.
Miner, C. S., & Dalton, N. N. (1953) *Glycerol*, p 271, Reinhold, New York.
Morales, M. F., Borejdo, J., Botts, J., Cooke, R., Mendelson, R. A., & Takashi, R. (1982) *Annu. Rev. Phys. Chem. 22*, 319-351.
Oster, G., & Adelman, A. H. (1956) *J. Am. Chem. Soc. 78*, 913-916.
Tonomura, Y., Appel, P., & Morales, M. F. (1966) *Biochemistry 5*, 515-521.
Uchida, K., Kato, S., & Koizumi, M. (1959) *Nature (London) 184*, 1620-1621.
Vanderkooi, J. M., & Berger, J. W. (1989) *Biochim. Biophys. Acta 976*, 1-27.
Venkataraman, B., Segal, B. G., & Fraenkl, G. K. (1959) *J. Chem. Phys. 30*, 1006-1017.
Weeds, A. G., & Taylor, R. S. (1975) *Nature (London) 257*, 54-56.
Zwicker, E. F., & Grossweiner, L. I. (1963) *J. Chem. Phys. 67*, 549-555.

Synthesis and Conformational Studies of N-Glycosylated Analogues of the HIV-1 Principal Neutralizing Determinant†

Ilona Laczkó,‡ Miklos Hollósi,§ Laszlo Ürge,∥ Kenneth E. Ugen,∥ David B. Weiner,∥ Henry H. Mantsch,⊥ Jan Thurin,∥ and Laszlo Ötvös, Jr.*,∥

Institute of Biophysics, Biological Research Center, 6701 Szeged, Hungary, Department of Organic Chemistry, L. Eötvös University, 1117 Budapest, Hungary, Steacie Institute for Molecular Sciences, National Research Council of Canada, Ottawa, Ontario, Canada K1A 0R6, and The Wistar Institute of Anatomy and Biology, 3601 Spruce Street, Philadelphia, Pennsylvania 19104

Received September 10, 1991; Revised Manuscript Received February 14, 1992

ABSTRACT: The principal neutralizing determinant (PND) of HIV-1 is found in the V_3 loop of the envelope glycoprotein. Antibodies elicited by peptides from this region, containing the GlyProGlyArgAlaPhe (GPGRAF) sequence, were able to neutralize diverse HIV-1 isolates [Javaherian et al. (1990) *Science 250*, 1590-1593]. The GPGR tetrapeptide was predicted to adopt a type II β-turn conformation. Earlier, we showed that glycosylation of synthetic T cell epitopic peptides at natural glycosylation sites stabilized β-turns [Ötvös et al. (1991) *Int. J. Pept. Protein Res. 38*, 467-482]. To evaluate the secondary structure modifying effect of the introduction of an N-glycosylated asparagine residue and to find a correlation between conformation and a possible PND potential, a series of glycopeptide derivatives, N(sugar)GPGRAFY-NH_2 (**4a-f**), have been prepared, together with the parent peptides GPGRAFY-NH_2 (**2**) and NGPGRAFY-NH_2 (**3**), by solid-phase peptide synthesis [sugars: (a) β-D-glucopyranosyl (Glc); (b) β-D-galactopyranosyl (Gal); (c) Glc-β(1→4)-Glc; (d) 2-acetamido-2-deoxy-β-D-glucopyranosyl (GlcNAc); (e) 2-acetamido-2-deoxy-β-D-galactopyranosyl (GalNAc); (f) GlcNAc-β(1→4)-GlcNAc; sugars are attached through a $\beta(1\rightarrow N^{\beta})$ linkage to asparagine (N).] Peptides **2-4** were characterized by amino acid analysis, reversed-phase HPLC, and fast atom bombardment mass spectrometry. Circular dichroism (CD) and Fourier-transform infrared (FT-IR) spectroscopic studies were performed in trifluoroethanol (TFE) and water (D_2O was used in FT-IR experiments). Nonglycosylated peptides showed significantly different CD spectra in aqueous and TFE solution. Moreover, a continuous spectral change was observed for all the peptides investigated when going from water to TFE. The chiral contribution of the aromatic side chains and acetamido sugars was also estimated. On the basis of CD and FT-IR evidence, the introduction of an N-glycosylated Asn residue does not destroy but rather stabilizes the suggested type II β-turn conformation of the PND peptide.

The principal neutralizing determinant (PND)[1] of HIV-1 is found in a disulfide-bridged loop (V_3) of the variable region of the envelope glycoprotein gp120 (LaRosa et al., 1990). Antibodies elicited to the amino acid backbone of PND peptides, containing the GlyProGlyArgAlaPhe (GPGRAF) sequence, were able to neutralize diverse HIV-1 isolates (Javaherian et al., 1990). This sequence was predicted to adopt a type II β-turn conformation encompassing the GPGR tetrapeptide (LaRosa et al., 1990). Since the PND sequence is surrounded by hypervariable regions at both sides, this type II β-turn structure is believed to be sensitive to environmental conditions.

† This work was supproted by NIH Grant GM 45011 (L.O.).
* Author to whom correspondence should be addressed.
‡ Institute of Biophysics, Biological Research Center.
§ Department of Organic Chemistry, L. Eötvös University.
∥ The Wistar Institute of Anatomy and Biology.
⊥ Steacie Institute for Molecular Sciences, National Research Council of Canada.

[1] Abbreviations: PND, principal neutralizing determinant; CD, circular dichroism; TFE, trifluoroethanol; FT-IR, Fourier-transform infrared; Glc, β-D-glucose; GlcNAc, 2-acetamido-2-deoxy-β-D-glucopyranose.

0006-2960/92/0431-4282$03.00/0